To Be or Not To Be… Cooperative? Trimetallic Catalysts for the Ring-Opening Polymerisation of Cyclic Esters

RESEARCH ARTICLE

To Be or Not To Be… Cooperative? Trimetallic Catalysts for the Ring-Opening Polymerisation of Cyclic Esters

Phoebe A. Lowy,[a] Maisarah Abdul Rahman,[a] Gary S. Nichol,[a] Carole A. Morrison[a] and Jennifer A. Garden*[a]

[a] P. A. Lowy, M. Abdul Rahman, Dr G. S. Nichol, Prof. C. A. Morrison, Dr J. A. Garden
EaStCHEM School of Chemistry
University of Edinburgh
Edinburgh, EH9 3FJ, United Kingdom
E-mail: j.garden@ed.ac.uk
URL: http://www.chem.ed.ac.uk/staff/academic-staff/dr-jennifer-garden

Supporting information for this article is given *via* a link at the end of the document.

Abstract: Multimetallic catalysts have emerged as a promising route to enhance catalyst performance in cyclic ester ring-opening polymerisation (ROP), as these complexes can outperform the monometallic analogues in terms of reactivity and/or polymerisation control. Such enhancements are often attributed to "multimetallic cooperativity", yet the origins of this cooperativity often remain unclear. Here, we report the synthesis and characterisation of two trimetallic Al-salen complexes (**L1(AlMe)$_3$** and **L1(AlEt)$_3$**), containing three Al-salen subunits in close proximity, and their monometallic analogues (**L2(AlMe)** and **L2(AlEt)**). These complexes have been applied as catalysts for cyclic ester ROP under a range of conditions, to probe their potential for cooperative behaviour. Trimetallic **L1(AlMe)$_3$** and **L1(AlEt)$_3$** both display high activities in *rac*-lactide ROP, giving k_{obs} values of up to 11 x 10^{-3} min^{-1}. Yet careful benchmarking against the monometallic complexes reveals that whether these systems display multimetallic cooperativity or not depends upon the reaction conditions. Detailed kinetic and spectroscopic studies into the origins of cooperativity revealed that the neighbouring metals play a key role in the initiation step, rather than propagation. Overall, these studies highlight the importance of understanding the reaction conditions in order to accurately define whether a catalyst displays multimetallic cooperativity.

Introduction

While "multimetallic cooperativity" has long been used by nature, such as naturally occurring bimetallic metalloenzymes,[1] this concept has been exploited relatively recently within catalyst design for cyclic ester ring-opening polymerisation (ROP). However, the number of multimetallic complexes reported is accelerating rapidly, as these catalysts often display enhanced catalyst activities and/or polymerisation control compared to the monometallic (single metal) analogues. For example, some multimetallic complexes have delivered improved control over the number-average molecular weight (M_n), dispersity ($Đ$) and stereocontrol of poly(lactic acid) (PLA), which is an industrially important bio-derived and biodegradable polymer.[2][3][4][5][6][7] Yet despite these advances, the origins of "multimetallic cooperativity" often remain unclear.

Within homogenous catalysis, multimetallic cooperativity is generally defined as an improved catalyst performance when using two or more metal centres per ligand framework, compared to the monometallic analogue(s). However, "cooperativity" is not always straightforward to determine. Drawing direct comparisons between mono- and multimetallic catalysts is challenging because there are often differences in the number of metal centres, the metal concentration, the metal-metal proximity, catalyst aggregation, metal coordination geometry, metal oxidation state and the number of initiating groups; all of these factors can influence the catalyst performance. This raises the question: is it fair to attribute enhanced activity to multimetallic cooperativity when so many other, often interlinking, factors are at play? To identify whether the metals in a multimetallic complex are acting cooperatively, it is important to assess whether the metals are working as a team, or conversely, if two metal centres both contribute to a process but act individually. In truly cooperative systems, the second metal may play a distinct role in the mechanism, or it may simply affect the electronic environment and thus the performance of the first metal.

Of the multimetallic catalysts reported for cyclic ester ROP, the majority have featured aluminium, as highlighted in a recent review article from Chen and co-workers.[8] Monometallic aluminium salen complexes featuring Al-alkoxide initiating units are well-established in *rac*-lactide (*rac*-LA) ROP and have delivered some of the highest levels of stereocontrol reported to date, yet often display moderate catalyst activities (e.g. **A1**, **Figure 1**).[9][10] Traditionally, the electronic environment of Al, and thus the catalyst performance, has been adjusted through modification of the ligand substituents. More recently, the incorporation of Mg or Zn as a second, heterometal was used to enhance the catalyst performance, by modulating the electronics of an Al-Cl initiating unit and by providing an additional site for monomer coordination (**B1** and **B2**, **Figure 1**).[11] Bimetallic aluminium systems, including examples based on salen ligands, have also shown good activities in cyclic ester ROP.[8][12][13]

Moving beyond bimetallic systems, trimetallic aluminium catalysts have been developed for cyclic ester ROP,[8][15] including elegant salen-derived catalysts reported by Chen and co-workers (e.g. **C1**, **Figure 1**).[14] These trimetallic complexes feature three salen subunits with three Al centres in a triangular arrangement, and delivered enhanced catalyst activity in both LA and ε-

caprolactone (ε-CL) ROP.[8][14] Impressively, **C1** was over 1125 times more active in LA ROP than the monometallic analogue (**D1**, **Figure 1**). This improvement was attributed to electronic communication between the three Al-salen subunits through the central phloroglucinol moiety.[16][17] This study is noteworthy as it not only demonstrates significant multimetallic cooperativity, but also enables a relatively direct comparison between the mono- and trimetallic complexes, as the metal centres are in identical coordination environments. Inspired by this work, we decided to synthesise two related tris-salen Al complexes (**L1(AlR)$_3$** (R = Me or Et), **Figure 1**). The ligand was adapted to include a phenylethylene diamine linker designed to further extend the conjugation and electronic communication within the ligand system, and a ketimine unit, which is more robust towards hydrolysis than the aldimine analogue.[18] Here, we probe whether these modified systems also exhibit multimetallic cooperativity, and whether cooperativity persists under a variety of reaction conditions, to determine the importance of reaction conditions in accessing and assessing multimetallic cooperativity.

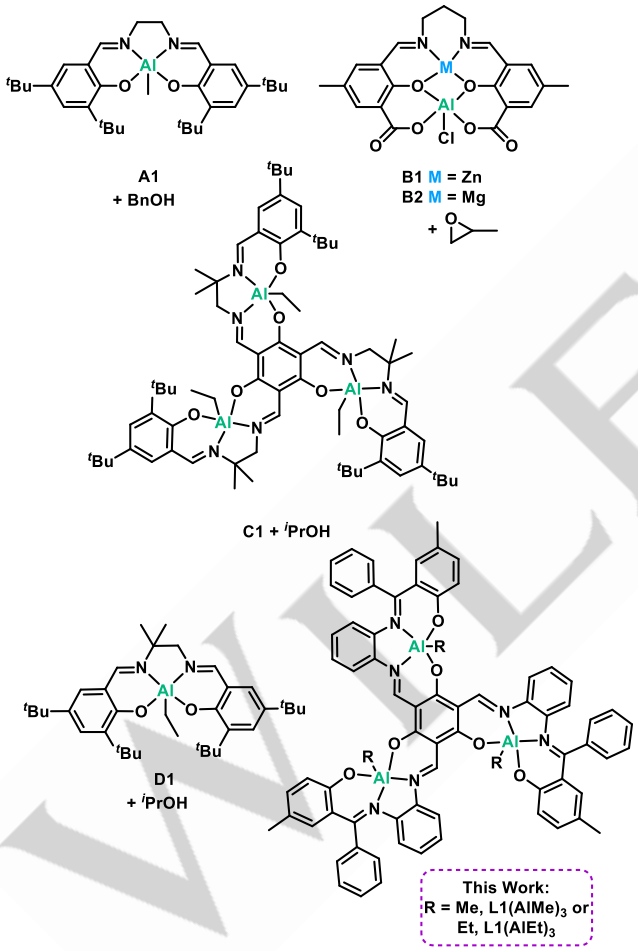

Figure 1. Examples of mono- and multimetallic aluminium-salen complexes reported for LA ROP, and the trimetallic complexes reported in this work.[10][11][14]

Results and Discussion

To synthesise the trimetallic aluminium complexes **L1(AlMe)$_3$** and **L1(AlEt)$_3$** along with their monometallic analogues **L2(AlMe)** and **L2(AlEt)**, asymmetric ligands **L1** and **L2** were prepared using adapted literature procedures (**Scheme 1**).[19] While the synthesis of symmetrical salen ligands is relatively straightforward and can be achieved through a one-pot Schiff-base condensation reaction, asymmetric salen ligands are more challenging to prepare.[20][21][22] The molecular structure of **L1** has previously been reported (refer to ESI for details),[19] and shows a loss of aromaticity in the central phloroglucinol unit as the ligand adopts the N-protonated tautomer instead of the expected OH-tautomer. This preference for the keto-enamine resonance form aligns with similar scaffolds reported in literature.[23][24] The ^{1}H NMR spectrum of **L1** provided further evidence for the loss of aromaticity, as the R(H)C-N*H* resonance was split into a doublet (13.46 ppm, J = 12.9 Hz); this was attributed to coupling from the imine N=C*H* proton (**Figure S1**).[25][26][27]

Upon addition of AlR_3 (where R = Me or Et), **L1** was converted into **L1(AlR)$_3$** as evidenced by the loss of the resonance at 13.46 ppm, as well as a significant downfield shift of the *H*C=N imine protons (from 8.49 ppm to 9.39 ppm for **L1(AlMe)$_3$** and 9.49 – 9.34 ppm for **L1(AlEt)$_3$**, **Figure S2** and **S4**). Both Al-alkyl groups in **L1(AlMe)$_3$** and **L1(AlEt)$_3$** displayed spectral splitting, which has been reported in literature for other tris-salen complexes. Here, a doublet of doublets was observed for **L1(AlMe)$_3$** (-0.97 ppm CH_3) and four resonances were observed for **L1(AlEt)$_3$** (CH_2CH_3, 0.81 and 0.71 ppm; CH_2, -0.23 and -0.29 ppm). Previous literature has attributed this spectral splitting to the flexibility of the M-alkyl group in tris-salen complexes, leading to different angles or orientations to the metal.[14][25]

Despite multiple attempts to crystallise these complexes, no suitable crystals for single crystal X-ray diffraction were obtained. Therefore, to probe the structural geometry of the aluminium tris-salen complex, a series of density-functional theory (DFT) calculations was performed for complex **L1(AlMe)$_3$** at the B3LYP/6-311G* level (see ESI). Four possible geometries were explored bearing different conformations with respect to the Al-methyl groups (**AlMe$_3$-I** – **AlMe$_3$-IV**, **Figure S11**). DFT studies suggest that the most stable configuration of **L1(AlMe)$_3$** features three aluminium metal centres in a twisted manner to form a "bowl-like" structure, with all three methyl groups pointing outward *i.e.*, on the convex face of the bowl (**L1(AlMe$_3$)-I**, see **Figure 2**). Switching the position of each methyl group in turn destabilises the structure, with ΔU rising by ca. 34.8 kJ mol^{-1} upon placement of all three Al-methyl groups "inside" the bowl (see ESI for details, **Table S1**). This higher energy conformation matches the general structural features observed in the crystal structure for a similar aluminium tris-salen complex **C1** (**Figure 1**), which showed all three Al-ethyl groups situated "inside" the bowl on the concave face.[14] This raises the question of whether intermolecular interactions in the solid state can act to stabilise the molecular conformation, and also whether solvent effects could play a similar role in solution. The complexity of the ^{1}H NMR spectra indicates that they do, as multiple sets of resonances are observed, indicating that different conformations are present in solution.[14][25] Aside from the molecular configuration, the calculations suggest that the local geometry around the three Al centres is almost identical, with each pentacoordinate Al occupying a distorted square pyramidal geometry ($\tau \cong 0.45$) and bonding to two N atoms (*ca.* 2.14 Å and 1.99 Å), two O atoms (*ca.* 1.80 Å and 1.89 Å) and one methyl group (*ca.* 1.97 Å).[28] The three Al centres are in a triangular arrangement with identical Al…Al distances of 7.41 Å and Al-Al-Al angles of 60°.

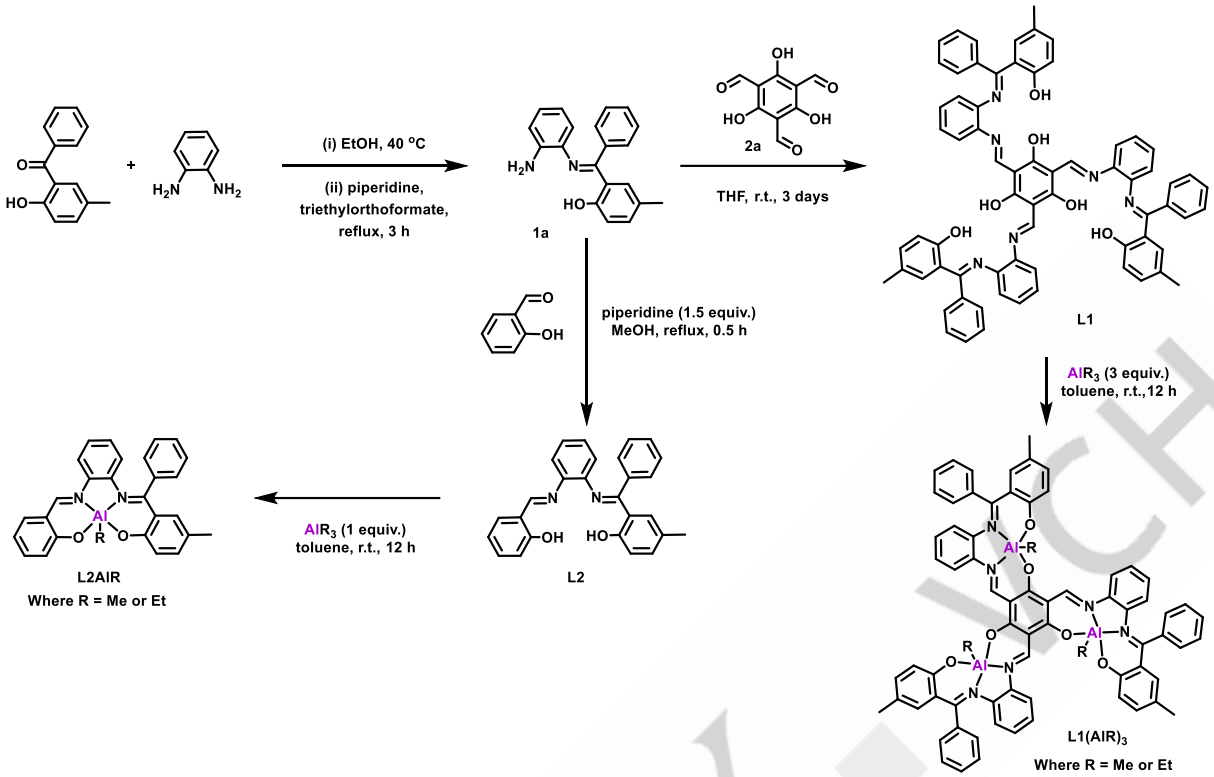

Scheme 1: General schematic for the preparations of ligands **L1** and **L2** and the subsequent metalation to generate **L1(AlMe)$_3$**, **L1(AlEt)$_3$**, **L2(AlMe)** and **L2(AlEt)**.

The Al…Al separation in **L1(AlMe)$_3$-I** is greater than in **C1**, where XRD analysis showed two unique complexes in the asymmetric unit with Al…Al distances of 6.38 Å and 6.40 Å and Al—Al—Al angles of 60.0° as imposed by the space group symmetry.[14]

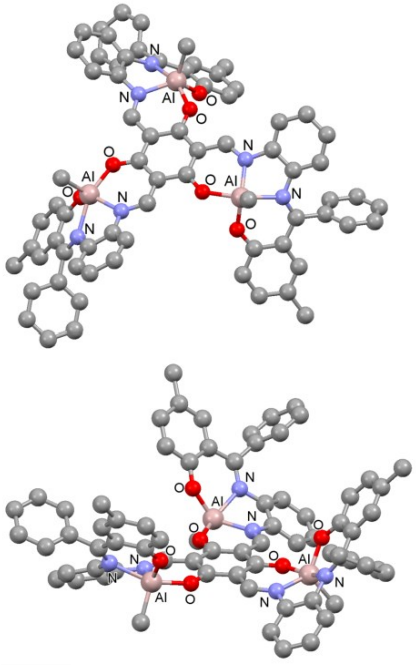

Figure 2. Top (top) and side view (bottom) of geometry optimised structure of the most stable configuration for complex **L1(AlMe)$_3$** (**L1(AlMe)$_3$-I**). H atoms are omitted for clarity. Colour scheme: grey = C, light purple= N, red = O, pink = Al.

Multimetallic cooperativity in cyclic ester ROP has been reported across M…M distances ranging from 2.8 – 8.0 Å,[8] although the optimal M…M distance appears to vary between different catalyst systems. As the Al…Al distance of **L1(AlMe)$_3$-I** falls within this range, it was of interest to investigate for potential multimetallic cooperativity.

For benchmarking purposes, the analogous mononucleating ligand **L2** was synthesised *via* the condensation reaction of 5-methyl-2-hydroxybenzophenone and *o*-phenylenediamine, followed by reaction with salicylaldehyde (**Scheme 1**). Subsequently, metallation with AlR_3 (where R = Me or Et, respectively) generated the monometallic Al-salen analogues **L2(AlMe)** and **L2(AlEt)**, as evidenced by loss of the phenolic resonances and a significant downfield shift of the *H*C=N imine protons (**Figure S3** and **S5**). All four Al-salen complexes were characterised by mass spectrometry, and DOSY NMR showed that the four complexes each display a monomeric structure in the solution-state (toluene-d_8, refer to ESI for details, **Figure S6** – **S9**).

The four Al-salen complexes were tested as catalysts for the ROP of *r*ac-LA at 70 °C in a toluene solution of 1M LA concentration (**Table 1**, **Figures S16** - **S39**). These conditions were selected as being optimum for related Al-salen structures,[14][29] and toluene was chosen as the solvent to improve the solubility of the Al catalysts. The complexes all displayed good activities towards LA ROP under certain conditions, albeit with very little stereocontrol as **L1(AlMe)$_3$** and **L2(AlMe)** generated mostly atactic PLA (P_s = 0.35 – 0.45, **Table S2**).

The tri- and mono-metallic aluminium methyl catalysts, **L1(AlMe)$_3$** and **L2(AlMe)**, were both inactive for LA ROP unless benzyl alcohol (BnOH) was added as an initiator (entries 3 and 6, **Table 1**). The alcoholysis of an unreactive Al-alkyl group to an effective Al-alkoxide initiating species has been well-established in LA ROP,[31][32] and thus monometallic Al-salen catalysts are typically used with one equivalent of an alcohol. Trimetallic **L1(AlMe)$_3$** features three potentially active metal centres.

Table 1. Ring-opening polymerisation of *rac*-LA with **L1(AlMe)$_3$**, **L1(AlEt)$_3$**, **L2(AlMe)** and **L2(AlEt)**:

Entry	Cat.	BnOH equiv.	LA equiv.	Pre stir (h)	Time (h)	[a]Conv (%)	[b] k_{obs} (x10^{-3} min^{-1})	[c] $M_{n\ calc}$ (kg mol^{-1}) (1 chain)	[d] $M_{n\ obs}$ (kg mol^{-1})	[e] $M_{n\ calc}$ (kg mol^{-1}) (3 chains)	$M_{n\ obs}$/ $M_{n\ calc}$ (1 chain)	$M_{n\ obs}$/ $M_{n\ calc}$ (3 chains)	*Đ*
1	**L1(AlMe)$_3$**	1	100	-	5	90	9.7	13.0	11.3	4.4	0.84	-	1.62
2	**L2(AlMe)**	1	100	-	5	47	4.5	6.8	5.8	-	0.85	-	1.21
3	**L1(AlMe)$_3$**	0	100	-	24	0	-	-	-	-	-	-	-
4	**L1(AlMe)$_3$**	3	300	-	5	64	5.0	25.9	9.2	8.6	0.34	1.02	1.15
5	**L1(AlMe)$_3$**	1	300	-	5	38	2.0	16.4	13.5	5.5	0.82	2.47	1.21
6	**L2(AlMe)**	0	100	-	24	0	-	-	-	-	-	-	-
7	**L1(AlEt)$_3$**	1	100	-	5	80	8.4	11.6	8.5	3.9	0.74	-	1.45
8	**L2(AlEt)**	1	100	-	5	89	9.2	12.9	7.9	-	0.62	-	1.67
9	**L1(AlEt)$_3$**	0	100	-	5	29	1.3	4.1	24.3	-	5.9	-	1.43
10	**L1(AlEt)$_3$**	3	300	-	5	45	3.1	19.3	6.0	6.5	0.32	0.95	1.13
11	**L2(AlEt)**	0	100	-	5	65	4.0	9.3	8.1	-	0.87	-	1.09
12	**L1(AlMe)$_3$**	1	100	1	2	67	9.4	9.6	12.2	3.2	1.2	-	1.30
13	**L1(AlMe)$_3$**	1	100	4	2	66	9.0	9.5	12.4	3.1	1.3	-	1.27
14	**L2(AlMe)**	1	100	4	2	66	9.4	9.5	8.2	-	0.86	-	1.41
15	**L1(AlEt)$_3$**	1	100	4	2	71	11.3	10.2	15.3	3.4	1.5	-	1.50
16	**L2(AlEt)**	1	100	4	2	87	17.5	12.5	4.8	-	0.38	-	1.97

Table 1: [*rac*-LA] = 1 M in toluene, 70 °C. [a]Conversion calculated using ^{1}H NMR spectroscopy. [b]Calculated from kinetic plots (refer to **Figures 3** and **4** and the ESI, **Figures S13 – S15**, for further details). Representative time points and the corresponding SEC data are included to enable direct comparisons between different catalysts and reaction conditions. [c]$M_{n,calc}$ of polymers calculated from the monomer conversion $M_{n,calc}$ = M_0 x ([M]/[I]) x conversion assuming 1 chain per catalyst. [d]$M_{n,obs}$ and *Đ* determined by size exclusion chromatography using polystyrene standards in THF. Values corrected by Mark-Houwink factor (0.58).[30] [e]$M_{n,calc}$ of polymers calculated from the monomer conversion $M_{n,calc}$ = M_0 x ([M]/[I]) x conversion assuming 3 chains per catalyst.

Here, kinetic studies and SEC analysis show that the number of equivalents of BnOH used dictates the number of active metal sites per catalyst. Specifically, when using 3 equivalents of BnOH, **L1(AlMe)$_3$** converted 300 equiv. of LA around 2.5 times faster than when only 1 equivalent of BnOH is used, giving respective k_{obs} values of 5.0 x 10^{-3} min^{-1} and k_{obs} = 2.0 x 10^{-3} min^{-1} (**Table 1** entry 4 *vs* entry 5, **Figure 3**). In addition to this, the M_n values determined by SEC analysis indicate that the BnOH activates all 3 metal centres, initiating 3 polymer chains, whereas only 1 chain is initiated when 1 equivalent is used (entries 4 and 5, **Table 1**).

The fastest rate for **L1(AlMe)$_3$** in LA ROP was observed using a [cat]:[BnOH]:[*rac*-LA] loading ratio of 1:1:100 (**Table 1**, entry 1). When only one metal centre was activated in trimetallic **L1(AlMe)$_3$**, the k_{obs} value was over double that of monometallic **L2(AlMe)** under identical conditions, with respective k_{obs} values of 9.7 x 10^{-3} min^{-1} and 4.5 x 10^{-3} min^{-1} (entries 1 and 2, **Table 1**, **Figure 3**). Furthermore, a test polymerisation, using **L1(AlMe)$_3$**, was performed at 0.33 M and compared to monometallic **L2(AlMe)** at 1 M, to bring the concentration of active Al centres for the mono- and trimetallic complexes into alignment (both with [cat]:[BnOH]:[*rac*-LA] = 1:1:100). At 0.33 M, **L1(AlMe)$_3$** displayed a higher LA conversion compared to **L2(AlMe)** at equivalent time points, despite the higher dilution of active Al centres (*i.e.* 32% LA conversion *vs* 23% LA conversion at 3 h, respectively). Together these results indicate that **L1(AlMe)$_3$** displays multimetallic cooperativity under both equivalent [catalyst] and [metal] concentrations, and that the non-activated Al centres can play a beneficial role in ROP. Interestingly, **L1(AlMe)$_3$** is twice as fast when one metal centre is activated compared to when all three metal centres are activated, with k_{obs} values of 9.7 x 10^{-3} min^{-1} *vs* 5.0 x 10^{-3} min^{-1} for consistent activated metal:*rac*-LA ratios of [cat]:[BnOH]:[*rac*-LA] = 1:1:100 or 1:3:300, respectively (entries 1 and 4). This observation also indicates that the non-activated neighbouring Al-Me centres in the trimetallic catalyst play a role in the polymerisation, hinting at multimetallic cooperativity.

However, when all three metal centres are activated, **L1(AlMe)$_3$** and **L2(AlMe)** show virtually identical rates of k_{obs} = 5.0 x 10^{-3} min^{-1} and 4.5 x 10^{-3} min^{-1}, respectively (entries 4 and 2, loading ratio [cat]:[BnOH]:[*rac*-LA] = 1:3:300 for **L1(AlMe)$_3$** and 1:1:100 for **L2(AlMe)**). These results suggest that each metal centre behaves identically when polymerising the same quantity of monomer (*i.e.* 100 equivalents of LA per active metal). This indicates that the Al centres in **L1(AlMe)$_3$** are acting individually, and are "uncooperative" in this system.

Taken together, these results show that the same multimetallic catalyst can be defined as "cooperative" or "uncooperative" depending on the reaction conditions and which sets of data are compared. When every metal centre is activated, the trimetallic and monometallic catalysts display similar rates, indicating the Al centres in **L1(AlMe)$_3$** are acting individually throughout the polymerisation. Yet when only one metal centre is activated per complex, the trimetallic catalyst is over twice as fast as its monometallic analogue (entries 1-2), indicating the influence of the inactive Al-Me centres. This raises the question: what role do the neighbouring Al-Me centres in **L1(AlMe)$_3$** play in increasing the catalyst activity?

Examining the kinetic data reveals an induction period for both **L1(AlMe)$_3$** and **L2(AlMe)** (**Figure 3**), and taking additional aliquots at early time points revealed that the induction period is

significantly shorter for trimetallic **L1(AlMe)$_3$** (**Figure 4(a)**). To probe the induction period in more detail, ^{1}H NMR spectroscopic monitoring of the reaction of **L1(AlMe)$_3$** and **L2(AlMe)** with BnOH was performed in toluene-d_8 at 70 ℃, to mimic the polymerisation conditions. The alcoholysis of the Al-Me units to form Al-OBn groups was confirmed through the loss of Al-alkyl and BnOH resonances and the formation of new benzoxide resonances (**Figure S39** and **S40**). Importantly, these studies revealed significant differences in the timescales of alcoholysis (**Figure 5**). With trimetallic **L1(AlMe)$_3$**, complete reaction of 1 equiv. of BnOH was observed after 15 mins (**Figure S39**). Conversely, even after 4 hours only 80 % of **L2(AlMe)** was converted to the active species **L2(AlOBn)**, as evidenced by unreacted **L2(AlMe)** and BnOH resonances (**Figure 5**, top trace and **Figure S40**).

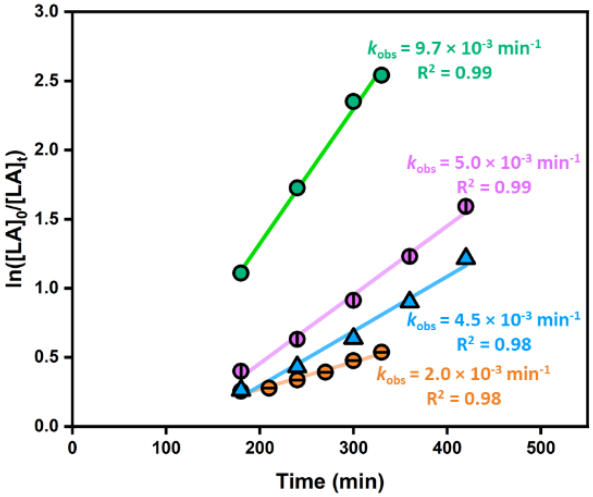

Figure 3. Semi-logarithmic plot of *rac*-LA conversion *vs* time at 70 ℃ with aluminium complexes **L1(AlMe)$_3$** and **L2(AlMe)** in toluene solvent with a loading ratio [cat]:[BnOH]:[*rac*-LA] = 1:1:100 unless stated otherwise: **L1(AlMe)$_3$** (k_{obs} = 9.7 x 10^{-3} min^{-1}), **L1(AlMe)$_3$** [cat]:[BnOH]:[*rac*-LA] = 1:3:300 (k_{obs} = 5.0 x 10^{-3} min^{-1}), **L2(AlMe)** (k_{obs} = 4.5 x 10^{-3} min^{-1}), **L1(AlMe)$_3$** [cat]:[BnOH]:[*rac*-LA] = 1:1:300 (k_{obs} = 2.0 x 10^{-3} min^{-1}).

The difference in initiation time between the tri- and mono-metallic complexes suggests that the additional aluminium centres in **L1(AlMe)$_3$** can either modulate the electronic environment of each Al-Me centre to make it more reactive towards BnOH, as has been observed with other tris-salen catalysts,[8][14] or can simply provide additional reactive Al-Me sites for alcoholysis. The ^{1}H NMR spectra of **L1(AlMe)$_3$** and **L2(AlMe)** show almost identical shifts for the Al-Me units (-0.97 ppm and -1.01 ppm, respectively), which indicates a similar electronic environment (**Figure S45**). The increased rate of formation of the active Al-OBn units is therefore likely to arise from the increased ratio of AlMe:BnOH with trimetallic **L1(AlMe)$_3$**. To overcome the differences in the initiation period, **L1(AlMe)$_3$** and **L2(AlMe)** were stirred with BnOH at 70 °C for 4 hours prior to polymerisation, to generate the active Al-benzoxide species. Upon incorporation of this "pre-stir", the propagation rates of **L1(AlMe)$_3$** and **L2(AlMe)** for LA ROP were brought into alignment (k_{obs} = 9.0 x 10^{-3} and 9.4 x 10^{-3} min^{-1} respectively, **Figure 4(b)**; entries 13 and 14, **Table 1**). Notably, pre-stirring **L1(AlMe)$_3$** with BnOH for just 1 hour, in line with the ^{1}H NMR monitoring studies, also gave a k_{obs} value of 9.4 x 10^{-3} min^{-1} (entry 12). Therefore, once the Al-alkyl group has been converted to the active Al-alkoxide initiator, the propagation rate is the same for both complexes ([cat]:[BnOH]:[*rac*-LA] = 1:1:100, toluene, 70 ℃). As the Al-Me groups do not initiate LA ROP (entries 3 and 6, **Table 1**), the slower rate of **L2(AlMe)** without a pre-stir is due to the slower activation of the aluminium metal centre. Therefore, the additional Al-Me centres present in the trimetallic complex do not display cooperative behaviour to aid or enhance propagation, but instead enhance the rate of alcoholysis, and therefore initiation.

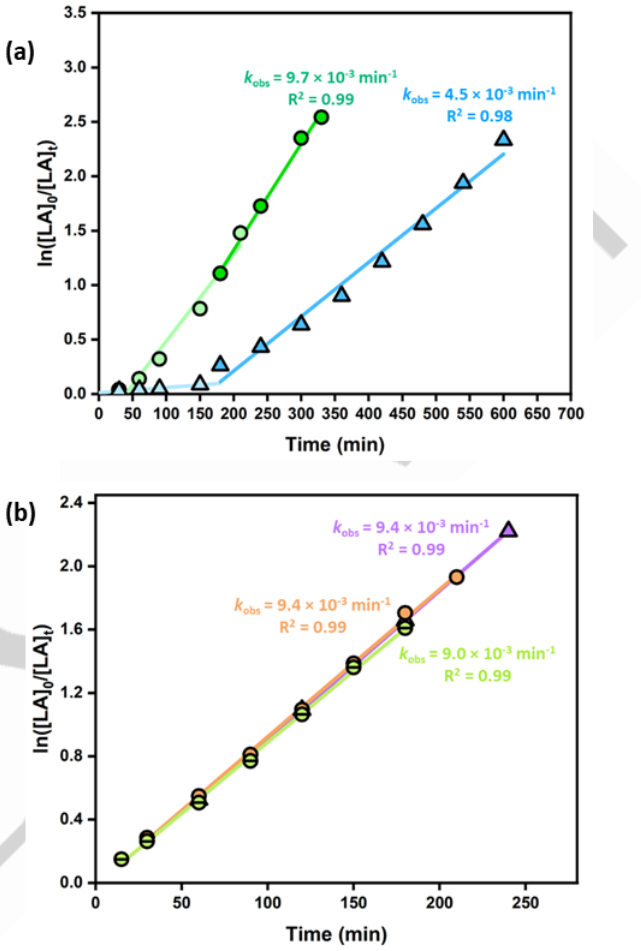

Figure 4. Semi-logarithmic plot of *rac*-LA conversion *vs* time at 70 ℃ to investigate the induction period with aluminium complexes **L1(AlMe)$_3$** and **L2(AlMe)** in toluene solvent with a loading ratio [cat]:[BnOH]:[*rac*-LA] = 1:1:100. **(a)** No pre-stir. **L1(AlMe)$_3$** (k_{obs} = 9.7 x 10^{-3} min^{-1}) and **L2(AlMe)** (k_{obs} = 4.5 x 10^{-3} min^{-1}) **(b)** **L1(AlMe)$_3$** (1 h pre stir, k_{obs} = 9.4 x 10^{-3} min^{-1}), **L2(AlMe)** (4 h pre stir, k_{obs} = 9.4 x 10^{-3} min^{-1}) and **L1(AlMe)$_3$** (4 h pre stir, k_{obs} = 9.0 x 10^{-3} min^{-1}).

Notably, there is literature precedent for the metal-metal proximity in bimetallic aluminium-salen catalysts to influence the behaviour towards alcohols. Firstly, Mazzeo and co- workers reported a series of bimetallic aluminium-salen catalysts, featuring linear propylene, pentylene or dodecylene diamine linker units.[12] As the shortest of the three, the propylene linker gave the fastest rate of alcoholysis with ^{i}PrOH and displayed no induction period, unlike the pentylene and dodecalene analogues. Secondly, salen complexes featuring an anthracene-1,8-diamine ("syn") or an anthracene-1,5-diamine ("anti") linker were reported. The "syn" conformation was noted to be more tolerant to the presence of excess BnOH than the "anti" conformation, which decomposed more readily.[13] Together with the data in this study, these observations start to build a picture of how the proximity of nearby metals may play a role in the reactivity of Al-alkyl units with alcohols. Providing further support for the similar reactivities of the mono- and tri-metallic complexes, the ^{1}H NMR spectra of the

reaction of **L1(AlMe)$_3$** or **L2(AlMe)** with 1 equiv. of BnOH at 1 or 4 hours, respectively, showed identical Al-OCH_2Ph resonances at 5.11 ppm (**Figure 5** and **S41**), indicating similar character of the initiating species in the mono- and tri-metallic complexes.

Overall these findings show that, without a detailed study, multimetallic cooperativity can easily be wrongly assigned. Here, the additional metal centres are only cooperative in that they enhance the rate of initiation, with no significant influence on the propagation rate.[13] The *in situ* alcoholysis of a metal-alkyl unit is a common route to initiate cyclic ester ROP, and this is often assumed to occur without the alcoholysis step having a significant impact on the catalyst performance. Yet this is not always the case, and some studies have reported reactivity differences between the isolated and *in situ* generated catalyst activities.[33][34] Here, we show that the active Al-alkoxide catalyst is not generated immediately for **L2(AlMe)**, and that differences in the formation of the active Al-alkoxide are in fact responsible for the activity differences between the mono- and tri-metallic catalysts.

In general, the number-average molecular weights determined by SEC analysis ($M_{n\ obs}$) gave good agreement with the theoretical values ($M_{n\ calc}$), indicating a relatively controlled polymerisation. Notably, the dispersity was slightly improved for trimetallic **L1(AlMe)$_3$** when the reaction conditions included a pre-stir with BnOH (entries 1, 12 and 13). In general, $M_{n\ obs}$ increased linearly with conversion, however in the late stages of the polymerisation $M_{n\ obs}$ deviated from $M_{n\ calc}$ and was lower than expected (**Figure S15 - S25**). End group analysis of PLA polymers by MALDI-ToF mass spectrometry showed the expected α-benzoxy, ω-hydroxy (major series) as well as α-hydroxy, ω-hydroxy (minor series) end-capped PLA (**Figure S46 - S51**). The latter series was attributed to chain transfer or transesterification reactions, increasing in the later stages of LA polymerisation as has been previously reported for other catalysts.[29][35] Overall, these results suggest that the polymerisation proceeds through a coordination−insertion mechanism mediated by the active M–OBn active species.

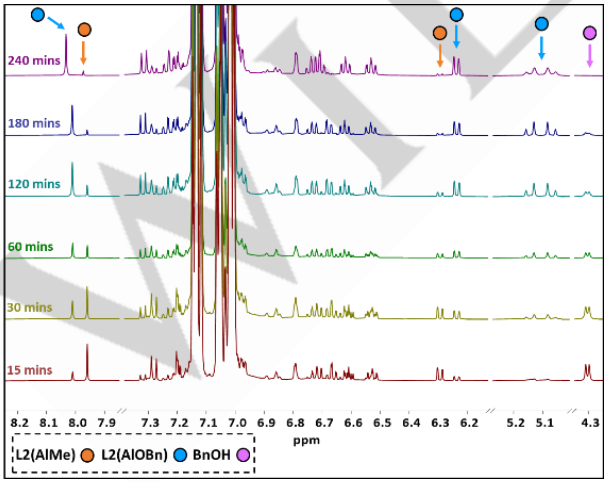

Figure 5. Key regions of the ^{1}H NMR spectra of the 1:1 reaction of **L2(AlMe)** and BnOH in toluene-d_8 over a 4 hour period.

Complex **L1(AlMe)$_3$** bears structural similarities to previously reported trimetallic Al-salen catalysts, which feature cyclohexyl or 1,1-dimethylethylene diamine linkers and various salicylaldehyde substituents at the 2- and 4-positions (**C1 – C2**, **Figure S52**).[14] While drawing exact comparisons between **L1(AlMe)$_3$**, **L2(AlMe)** and **C1 - C2** is somewhat limited by the range of polymerisation conditions used, **L1(AlMe)$_3$** displayed competitive activities compared to **C1** and **C2** (**Figure S52**). However, a key difference is that trimetallic **C1 – C2** display a much more significant activity enhancement compared to their monometallic analogues **D1** and **D2**, which are much less active than **L2(AlMe)** (see ESI).

The Al-Et complexes **L1(AlEt)$_3$** and **L2(AlEt)** were also active towards LA ROP and displayed good activities (**Table 1**, entries 7 – 11 and 15 – 16). The Al-Et complexes could be expected to be more Brønsted basic (favouring alcoholysis) and nucleophilic (favouring LA ring-opening) than their Al-Me counterparts (**Figure S44**); previously reported Al-Et complexes have outperformed their Me-substituted analogues.[36][37][38] Indeed, in contrast to the Al-Me analogues, **L1(AlEt)$_3$** is active in the absence of BnOH albeit with poor initiation efficiency as indicated by polymers of unexpectedly high molecular weight and relatively broad dispersity (entries 3 and 9, **Table 1**). In the presence of BnOH, **L1(AlEt)$_3$** and **L1(AlMe)$_3$** showed similar activities (**Table 1**, entries 1 and 7). Kinetic studies as well as ^{1}H NMR spectroscopic analysis showed the alcoholysis of **L1(AlEt)$_3$** took ~4 hours instead of the 15 mins required for **L1(AlMe)$_3$** ([cat]:[BnOH]:[*rac*-LA] = 1:1:100, **Figure S41** and **S42**). Incorporating a pre-stir gave similar k_{obs} values for **L1(AlEt)$_3$** and **L1(AlMe)$_3$** (11.3 x 10^{-3} and 9.4 x 10^{-3} min^{-1}, respectively), indicating that the remaining, unreacted Al-Et or Al-Me units have little impact on the polymerisation rate (**Figure 6**).

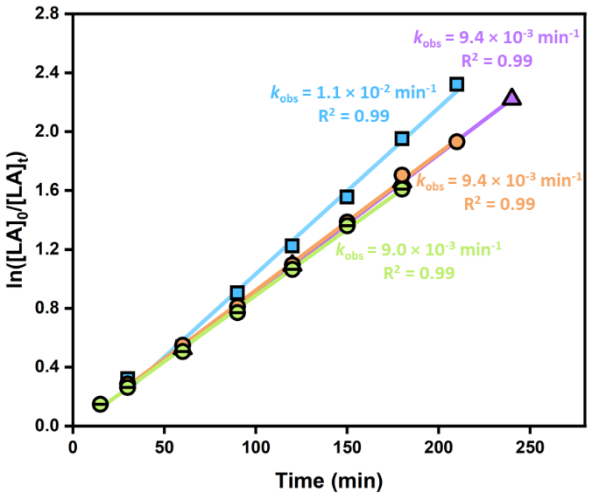

Figure 6. Semi-logarithmic plot of *rac*-LA conversion *vs* time at 70 °C with aluminium complexes **L1(AlMe)$_3$**, **L2(AlMe)** and **L1(AlEt)$_3$** following a "pre-stir" with BnOH in toluene solvent with a loading ratio as following [cat]:[BnOH]:[*rac*-LA] = 1:1:100, **L1(AlMe)$_3$** (1 h pre stir, k_{obs} = 9.4 x 10^{-3} min^{-1}), **L1(AlEt)$_3$** (4 h pre stir, k_{obs} = 11.3 x 10^{-3} min^{-1}), **L2(AlMe)** (4 h pre stir, k_{obs} = 9.4 x 10^{-3} min^{-1}), **L1(AlMe)$_3$** (4 h pre stir, k_{obs} = 9.0 x 10^{-3} min^{-1}).

Notably, when pre-stirred with BnOH for 4 hours, monometallic **L2(AlEt)** displayed the highest catalytic activity of all (entry 16, k_{obs} = 17.5 x 10^{-3} min^{-1}), albeit with poor control over the molecular weight and broad dispersities. Intriguingly, pre-stirred **L2(AlEt)**/BnOH is twice as active as pre-stirred **L2(AlMe)**/BnOH (k_{obs} = 17.5 x 10^{-3} min^{-1} *vs* k_{obs} = 9.4 x 10^{-3} min^{-1} respectively, entries 16 and 14). ^{1}H NMR monitoring studies of the reaction between **L2(AlEt)** and BnOH show that the reaction is incomplete even after 24 h (**Figure S43**). Moreover, **L2(AlEt)** is capable of

initiating LA ROP in the absence of BnOH, unlike **L2(AlMe)** (entries 6 and 11). Therefore, the difference in activity between **L2(AlEt)**/BnOH and **L2(AlMe)**/BnOH is attributed to incomplete alcoholysis and the potential for other, competing initiation processes for **L2(AlEt)**.

All four mono- and tri-metallic aluminium complexes were active in ε-CL ROP (**Table 2**), and were first order with respect to monomer concentration (**Figures 7(a)** and **(b)**). Unlike LA ROP, all four complexes were active without BnOH although significantly higher polymerisation rates were observed with BnOH (e.g. entries 1 *vs* 3, **Table 2**). Both **L1(AlMe)$_3$** and **L1(AlEt)$_3$** displayed similar propagation rates for ε-CL ROP under identical conditions (**Figures 7(a)** and **(b)**), and also showed relatively similar induction periods, unlike for LA ROP (**Figure 7(a)** for ε-CL *vs* **Figure 4(a)** for LA). The greater similarity between **L1(AlMe)$_3$** and **L1(AlEt)$_3$** in ε-CL ROP, compared to LA ROP, may be because both can initiate in the absence of BnOH. The shorter initiation period also indicates the possibility of an activated monomer mechanism, where BnOH acts as an exogeneous initiator to ring-open an Al-coordinated CL monomer.[39][40]

Table 2. Kinetic studies of ε-CL ROP with **L1(AlMe)$_3$**, **L1(AlEt)$_3$**, **L2(AlMe)** and **L2(AlEt)**:

Entry	Cat.	BnOH equiv.	ε-CL equiv.	Pre stir (h)	Time (min)	[a]Conv (%)	[b]k_{obs} (x10^{-2} min^{-1})	[c] $M_{n\ calc}$ (kg mol^{-1}) (1 chain)	[d] $M_{n\ obs}$ (kg mol^{-1})	[e] $M_{n\ calc}$ (kg mol^{-1}) (3 chains)	$Đ$
1	**L1(AlMe)$_3$**	1	100	-	45	97	7.4	11.0	14.5	3.7	1.45
2	**L2(AlMe)**	1	100	-	45	83	6.2	9.5	4.0	-	1.39
3	**L1(AlMe)$_3$**	0	100	-	60	10	-	-	-	-	-
4	**L2(AlMe)**	0	100	-	180	71	-	8.1	11.4	-	2.04
5	**L1(AlMe)$_3$**	3	300	-	45	98	8.6	31.9	5.9	10.6	2.13
6	**L1(AlEt)$_3$**	1	100	-	60	98	8.3	11.2	6.6	3.8	1.88
7	**L2(AlEt)**	1	100	-	60	89	3.8	10.1	3.2	-	2.92
8	**L1(AlEt)$_3$**	0	100	-	60	35	1.2	4.0	21.4	1.3	1.84
9	**L2(AlEt)**	0	100	-	60	35	0.7	4.0	64.0	-	2.57
10	**L1(AlEt)$_3$**	3	300	-	60	87	4.5	29.7	5.2	9.9	2.49
11	**L1(AlMe)$_3$**	1	100	1[f]	10	91	24.5	10.4	3.9	3.4	2.50
12	**L2(AlMe)**	1	100	4[f]	10	75	14.3	8.5	2.6	-	2.06
13	**L1(AlEt)$_3$**	1	100	4[f]	10	92	24.6	10.4	4.0	3.4	2.53
14	**L2(AlEt)**	1	100	4[f]	10	61	9.8	7.0	2.9	-	2.23

Table 2: [ε-CL] = 1 M in toluene, 70 °C. [a]Conversion calculated using ^{1}H NMR spectroscopy. [b]Calculated from kinetic plots (refer to **Figures 7(a)** and **7(b)** and the ESI for further details). Representative time points and the corresponding SEC data are included to enable direct comparisons between different catalysts and reaction conditions. [c]$M_{n,calc}$ of polymers calculated from the monomer conversion $M_{n,calc}$ = M_0 x ([M]/[I]) x conversion assuming 1 chain per catalyst. [d]$M_{n,obs}$ and $Đ$ determined by size exclusion chromatography using polystyrene standards in THF. Values corrected by Mark-Houwink factor (0.56).[43] [e]$M_{n,calc}$ of polymers calculated from the monomer conversion $M_{n,calc}$ = M_0 x ([M]/[I]) x conversion assuming 3 chains per catalyst. [f] Reaction time based on the ^{1}H NMR monitoring studies of the catalyst with BnOH in toluene-d_8 at 70 °C (*vide supra*).

In the presence of 1 equivalent of BnOH, trimetallic **L1(AlMe)$_3$** and monometallic **L2(AlMe)** display similar rates in ε-CL ROP, which suggests a lack of multimetallic cooperativity (respective k_{obs} values of 7.4 x 10^{-2} min^{-1} and 6.2 x 10^{-2} min^{-1}, [cat]:[BnOH]:[*rac*-LA] = 1:1:100, **Figure 7(a)**). SEC and MALDI-ToF analysis showed that the polymerisation was relatively well-controlled in the early stages of the polymerisation, with α-benzoxy, ω-hydroxy-end capped PCL observed as the major species (see ESI). Yet during the late stages of polymerisation a greater deviation from $M_{n\ calc}$ was observed (**Table 2**, see ESI), attributed to transesterification reactions and/or competing mechanisms occurring (*i.e.* activated monomer and coordination-insertion).[41]

Previous studies have shown that some metal complexes can operate simultaneously through these two different ROP mechanisms, contributing to poor polymerisation control.[31][39][42] To probe whether multimetallic cooperativity occurred in ε-CL ROP after conversion to the aluminium-benzoxide species, all four complexes were investigated following a pre-stir with BnOH, which significantly increased the propagation rate in all four cases (**Table 2**, entries 11 – 14, **Figure 7(b)** *vs* **7(a)**). For example, the propagation rate of trimetallic **L1(AlMe)$_3$** was increased from 7.4 x 10^{-2} min^{-1} to 24.5 x 10^{-2} min^{-1} (entries 1 and 11), albeit with poorer polymerisation control (entries 11 – 14, **Table 2**, see ESI). Following a "pre-stir" with BnOH, trimetallic **L1(AlMe)$_3$** and **L1(AlEt)$_3$** gave identical rates (**Figure 7(b)**), and similar molecular weights and dispersities ($M_{n\ obs}$ = 3.9 kg mol^{-1} and 4.0 kg mol^{-1}, $Đ$ = 2.50 and 2.53 respectively), which shows that the residual Al-alkyl groups do not significantly impact the catalyst activity. Notably, the activities of the trimetallic complexes are almost double those of the monometallic catalysts once pre-activated with 1 equiv. of BnOH, which hints at multimetallic cooperativity (entries 11 – 14, **Figure 7(b)**). This may arise from electronic communication through the central phloroglucinol core, as has been reported for other tris-salen complexes.[8][14] Taken together, these results reinforce that the assignment of multimetallic cooperativity can depend on the reaction conditions used.

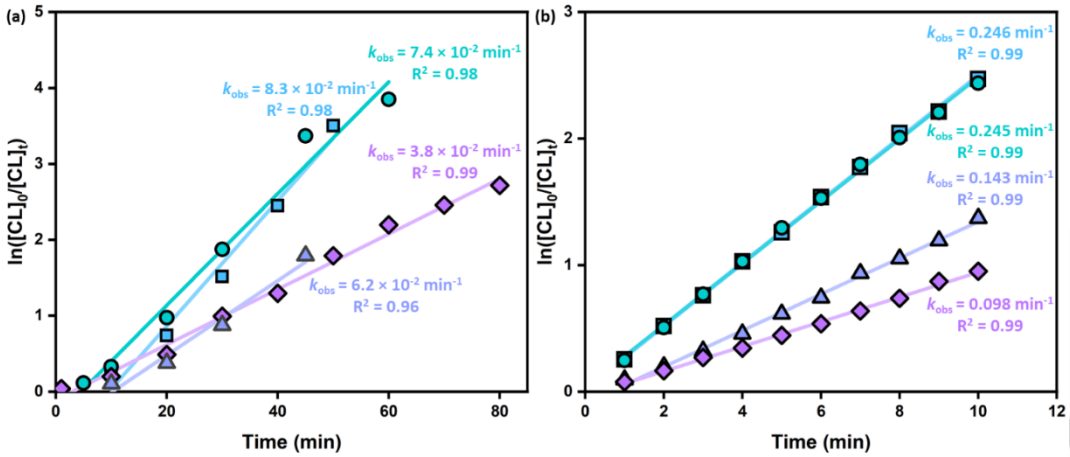

Figure 7: Semi-logarithmic plot of ε-CL conversion *vs* time at 70 °C with aluminium complexes **L1(AlMe)$_3$**, **L1(AlEt)$_3$**, **L2(AlMe)** or **L2(AlEt)** in toluene solvent with loading ratios of [cat]:[BnOH]:[ε-CL] = 1:1:100. Plot **(a)** shows kinetic plots without pre-stirring the catalyst with BnOH; plot **(b)** shows the kinetic plots after pre-stirring the catalyst with BnOH (b). **(a)** **L1(AlEt)$_3$** (k_{obs} = 8.3 x 10^{-2} min^{-1}), **L1(AlMe)$_3$** (k_{obs} = 7.4 x 10^{-2} min^{-1}), **L2(AlMe)** (k_{obs} = 6.2 x 10^{-2} min^{-1}) and **L2(AlEt)** (k_{obs} = 3.8 x 10^{-2} min^{-1}). **(b)** **L1(AlEt)$_3$** (4 h pre stir, k_{obs} = 0.246 min^{-1}), **L1(AlMe)$_3$** (1 h pre stir, k_{obs} = 0.245 min^{-1}), **L2(AlMe)** (4 h pre stir, k_{obs} = 0.143 min^{-1}) and **L2(AlEt)** (4 h pre stir, k_{obs} = 0.098 min^{-1}).

Conclusion

Overall, these studies report four aluminium-salen complexes and investigate reactivity differences between mono- and tri-metallic complexes. Importantly, these results show that the trimetallic complexes display multimetallic cooperativity under some reaction conditions, but not all. For example, while initial results benchmarking **L1(AlMe)$_3$** against **L2(AlMe)** indicated different activities in LA ROP and multimetallic cooperativity within **L1(AlMe)$_3$**, detailed kinetic and ^{1}H NMR spectroscopy studies show that the cooperativity only occurs in the initiation stage, by assisting the conversion of inactive Al-alkyl groups into active Al-alkoxide units. Once activated, the mono- and tri-metallic catalysts give identical activities. This is a key finding, as the *in situ* activation of metal-alkyl bonds using alcohols is a widely used method of initiating ROP and has sometimes been used to test catalyst activity without investigation into the initiation period. These studies highlight the importance of testing multimetallic catalysts under different conditions instead of using single time points, as has sometimes been reported in literature, to avoid mis-assigning activity differences to multimetallic cooperativity within the propagation step.

Experimental Section

^{1}H, ^{13}C, and 2D NMR (COSY, HSQC) spectra were recorded on Bruker AVA500, PRO500 and AVA400 spectrometers at 298 K (500 MHz for ^{1}H and 126 MHz for ^{13}C). The DOSY plot was generated using the DOSY processing module of TopSpin. Parameters were optimised empirically to find the best quality of data for explanation purposes. For SEC analyses, polymer samples (2 – 10 mg) were dissolved in GPC grade THF (1 ml) and filtered using a 0.2 µm PTFE syringe filter. SEC analyses of the filtered polymer samples were carried out in SEC grade THF at a flow rate of 1 ml min^{-1} at 35 °C on a 1260 Infinity II GPC/SEC single detection system with mixed bed C PLgel columns (300 x 7.5 mm). The RI detector was calibrated using narrow molecular weight polystyrene standards. APPI-MS analysis was performed using a Bruker Daltonics 12T SolariX Fourier Transform Ion Cyclotron Resonance Mass Spectrometer using atmospheric pressure photoionisation (APPI). Mass spectrometry analysis was carried out using nominal mass electron ionisation mass spectrometry in the positive ion mode, collected on a Thermo Fisher Scientific TRACE™ GC Ultra gas chromatograph. MALDI-ToF MS analyses were performed using a Bruker Daltonics UltrafleXtreme™ MALDI-ToF/ToF MS instrument. The sample to be analysed, dithranol matrix and KI (cationising agent) were dissolved in THF at 10 mg ml^{-1} and the solutions were mixed in a 2:2:1 volume ratio, respectively. A droplet (2 µl) of the resultant mixture was spotted on to the sample plate and submitted for MALDI-ToF MS analysis.

All manipulations involving air or water sensitive compounds were performed either in a glove box or using standard Schlenk techniques under an argon atmosphere. All reagents and solvents were obtained from Merck, Fisher Scientific, Honeywell and Fluorochem Ltd. and used without further purification unless stated otherwise. Dry solvents (THF and toluene) were collected from a solvent purification system (Innovative Technologies), dried over activated 4 Å molecular sieves and stored under argon. $CDCl_3$ and toluene-d_8 solvents for NMR spectroscopy studies were degassed by three freeze−pump−thaw cycles and stored over activated 4 Å molecular sieves under an argon atmosphere. *Rac*-lactide (*rac*-LA) was purified by double recrystallisation from toluene followed by sublimation. Benzyl alcohol (BnOH) and ε-caprolactone (ε-CL) were dried over CaH_2 and distilled under reduced pressure prior to use.

Synthesis of Ketimine Half Unit **1a**

The salen half unit **1a** (Scheme 1) was prepared according to an adapted literature procedure.[19] 5-Methyl-2-hydroxybenzophenone (3.00 g, 14.13 mmol) and 1,2-phenylenediamine (1.56 g, 14.43 mmol) were suspended in ethanol (10 ml). This suspension was stirred at 40 °C until an orange solution formed. Piperidine (1.50 ml, 15.18 mmol) and triethylorthoformate (3.00 ml, 18.06 mmol) were added. The reaction mixture was heated at reflux for 3 h. The solution was cooled to room temperature and put in the freezer overnight, and

orange needles were deposited from solution. The precipitate was collected by filtration, washed with ice cold ethanol (20 ml), and dried *in vacuo* to yield orange crystals (1.40 g, 32%). The ^{1}H NMR and ^{13}C NMR spectra of the products were consistent with reported literature values.[19]

^{1}H NMR (500 MHz, Chloroform-*d*): δ 14.15 (s, 1H), 7.38 – 7.27 (m, 3H), 7.24 – 7.16 (m, 3H), 6.99 (d, *J* = 8.4 Hz, 1H), 6.87 (dd, *J* = 2.2, 0.8 Hz, 1H), 6.86 – 6.79 (m, 1H6.68 (dd, *J* = 7.9, 1.3 Hz, 1H), 6.41 (td, *J* = 7.6, 1.3 Hz, 1H), 6.26 (dd, *J* = 7.9, 1.4 Hz, 1H), 3.82 (s, 2H), 2.17 (s, 3H).**^{13}C NMR (126 MHz, Chloroform-*d*):** δ 175.3, 160.3, 139.3, 134.5, 134.3, 134.2, 132.2, 129.2, 128.5, 128.3, 127.3, 125.8, 122.0, 119.8, 118.1, 117.8, 115.2, 20.6.

ESI-MS: m/z [M+H]$^{+}$: calculated 303.14; **found 303.14**

Synthesis of 2,4,6-Trihydroxybenzene-1,3,5-tricarbaldehyde **2a**
2,4,6-Trihydroxybenzene-1,3,5-tricarbaldehyde **2a** was prepared according to a modified literature procedure.[44] Under a N_2 atmosphere, trifluoroacetic acid (45 ml) was added to a mixture of phloroglucinol (3.00 g, 23.8 mmol) and hexamethyltetraamine (7.34 g, 52.36 mmol) and stirred at 100 ℃ for 3 h. To this, 3 M HCl was slowly added and the reaction mixture was stirred at 100 ℃ for 1 h. The solution was left to cool to room temperature, stored in a freezer overnight, and then filtered *via* a Buchner funnel. The filtrate was washed with ice cold water (3 x 20 ml) followed by $CHCl_3$ (100 ml). The $CHCl_3$ contained the product, and was concentrated *in vacuo* to yield a white solid (857.6 mg, 8 %). ^{1}H and ^{13}C NMR spectra of the product were consistent with reported literature values.[44]

^{1}H NMR (500 MHz, Chloroform-*d*): δ 14.12 (s, 3H), 10.15 (s, 3H).

^{13}C NMR (126 MHz, $CDCl_3$): δ 192.20, 173.73, 103.03.

Synthesis of Tris-Salophen Ligand **L1**
L1 was prepared according to an adapted literature procedure.[19] **1a** (0.21 g, 1.00 mmol) and **2a** (1.81 g, 5.99 mmol) were dissolved in tetrahydrofuran (30 ml). The resulting orange solution was stirred at room temperature for 3 days, during which time a yellow precipitate formed. The precipitate was collected by filtration, washed with methanol (30 ml), and dried *in vacuo*. **L1** was isolated as a bright yellow solid (710.2 mg, 67 %). The product was characterised through a combination of multinuclear NMR (^{1}H, ^{13}C, COSY, HSQC) spectroscopy, ESI mass spectrometry and single crystal X-ray diffraction. The ^{1}H and ^{13}C NMR spectra were consistent with literature.[19]

^{1}H NMR (500 MHz, $CDCl_3$): δ 13.52 (s, 3H), 13.46 (d, *J* = 12.9 Hz, 3H), 8.49 (d, *J* = 12.8 Hz, 3H), 7.28 (ddd, *J* = 6.6, 4.5, 2.4 Hz, 9H), 7.23 (dd, *J* = 8.5, 1.5 Hz, 5H), 7.14 – 7.06 (m, 9H), 7.02 (td, *J* = 7.8, 1.5 Hz, 4H), 6.91 – 6.83 (m, 6H), 6.58 (dd, *J* = 7.9, 1.4 Hz, 3H), 2.18 (s, 9H).

^{13}C NMR (126 MHz, Chloroform-*d*): δ 185.4, 177.5, 160.8, 148.4, 138.6, 134.8, 134.5, 132.8, 131.7, 129.3, 128.4, 128.2, 127.1, 125.6, 124.8, 123.1, 119.8, 118.05, 115.4, 107.7.

ESI-MS: m/z [M+H]$^{+}$: calculated 1063.41; **found 1063.42**

X-ray crystallographic data and refinement details for L1
(note that X-ray crystallographic data for L1 has been previously reported in literature[19]): $C_{74}H_{66}N_6O_6$, M_r = 1135.32, trigonal, *P*-3, a = 17.8396(11) Å, b = 17.8396(11) Å, c = 10.9900(10) Å, α = 90°, β = 90°, γ = 120°, *V* = 3029.0(5) Å^3, *T* = 100.1 K, *Z* = 2, *Z'* = 0.333333, μ(MoK_α) = 0.080, 73913 reflections measured, 4144 unique (R_{int} = 0.0529) which were used in all calculations. The final wR_2 was 0.1010 (all data) and R_1 was 0.0367 (I≥2 σ(I)).

Synthesis of Mono-Salophen Ligand **L2**
L2 was prepared according to an adapted literature procedure.[19] Salicylaldehyde (0.20 ml, 1.03 mmol) was added dropwise to a solution of the ketimine half unit (302.8 mg, 1 mmol) in MeOH (5 ml). Piperidine (0.15 ml, 1.56 mmol) was added to the suspension and the mixture was refluxed for 0.5 hours. On cooling to room temperature the yellow precipitate formed was collected by filtration, washed with MeOH (10 ml) and dried *in vacuo* to yield a bright yellow solid (304.6 mg, 75 %).

^{1}H NMR (500 MHz, $CDCl_3$): δ 13.82 (s, 1H), 12.97 (s, 1H), 8.38 (s, 1H), 7.33 (ddd, *J* = 15.2, 8.3, 1.7 Hz, 2H), 7.29 – 7.23 (m, 1H), 7.23 – 7.15 (m, 3H), 7.10 – 7.01 (m, 5H), 7.01 (d, *J* = 8.5 Hz, 1H), 6.97 (dd, *J* = 8.2, 1.1 Hz, 1H), 6.91 (td, *J* = 7.5, 1.1 Hz, 1H), 6.83 – 6.75 (m, 2H), 2.14 (s, 3H).

^{13}C NMR (126 MHz, Chloroform-*d*): δ 174.60, 162.48, 161.26, 160.47, 141.97, 139.95, 134.74, 134.41, 133.15, 132.18, 132.17, 128.85, 128.40, 127.84, 126.91, 125.37, 123.17, 119.36, 119.20, 118.89, 118.47, 117.92, 117.48, 20.53.

ESI-MS: m/z [M+H]$^{+}$: calculated 407.17; **found 407.18**

Synthesis of Tris-Al-Salophen Complex **L1(AlMe)$_3$**
To a suspension of **L1** (150 mg, 0.14 mmol) in toluene (12 ml), a solution of $AlMe_3$ (0.23 ml, 0.42 mmol) in toluene (8 ml) was added dropwise. The solution was stirred at room temperature for 12 h before being concentrated *in vacuo* to yield a red solid (122.0 mg, 74 %).

^{1}H NMR (500 MHz, $CDCl_3$): δ 9.39 (dd, *J* = 11.7, 6.7 Hz, 3H), 7.60 – 7.47 (m, 12H), 7.26 – 7.21 (m, 1H), 7.20 – 7.12 (m, 9H), 7.05 (dd, *J* = 8.4, 2.2 Hz, 2H), 6.96 (dd, *J* = 8.5, 4.0 Hz, 2H), 6.87 – 6.69 (m, 6H), 6.38 – 6.32 (m, 3H), 2.15 – 2.07 (m, 9H), -0.97 (dd, *J* = 25.7, 3.7 Hz, 9H).

^{13}C NMR (126 MHz, $CDCl_3$): δ 177.10, 172.07, 157.39, 157.16, 156.74, 137.88, 137.61, 136.81, 136.75, 136.58, 133.16, 133.04, 129.36, 129.28, 127.93, 127.83, 125.49, 125.46, 125.30, 125.16, 123.56, 123.02, 122.85, 117.13, 117.02, 105.91, 20.58, 20.53.

(APPI-MS): *m/z* [M+H]$^{+}$: calculated 1183.38; **found 1183.40**

Synthesis of Mono-Al-Salophen Complex **L2(AlMe)**
To a suspension of **L2** (300 mg, 0.74 mmol) in toluene (12 ml), a solution of $AlMe_3$ (0.39 ml, 0.74 mmol) in toluene (8 ml) was added dropwise. The solution was stirred at room temperature for 12 h before being concentrated *in vacuo* to yield a yellow solid (288.0 mg, 87 %).

^{1}H NMR (500 MHz, $CDCl_3$): δ 8.63 (s, 1H), 7.55 – 7.41 (m, 5H), 7.36 (dd, *J* = 7.8, 1.9 Hz, 1H), 7.28 – 7.17 (m, 3H), 7.10 (dd, *J* =

8.6, 1.7 Hz, 2H), 6.88 (ddd, *J* = 8.7, 7.5, 1.3 Hz, 1H), 6.82 – 6.74 (m, 2H), 6.41 (dd, *J* = 8.4, 1.2 Hz, 1H), 2.11 (s, 3H), -0.99 (s, 3H).

^{13}C NMR (126 MHz, $CDCl_3$): δ 173.94, 166.88, 164.64, 160.60, 139.83, 138.76, 137.56, 136.71, 135.78, 133.60, 132.95, 129.52, 129.04, 128.72, 128.23, 127.41, 127.11, 125.30, 124.98, 124.09, 123.13, 123.03, 119.79, 119.18, 116.86, 116.41, 77.21, 31.59, 22.66, 21.46, 20.51, 14.12, 1.02.

(APPI-MS): *m/z* $[M+H]^+$: calculated 447.16; **found 447.17**

Synthesis of Tris-Al-Salophen Complex **L1(AlEt)$_3$**
To a suspension of **L1** (150 mg, 0.14 mmol) in toluene (12 ml), a solution of $AlEt_3$ (48 mg, 0.42 mmol,) in toluene (4 ml) was added dropwise. The solution was stirred at room temperature overnight before being concentrated *in vacuo* to yield a red solid (148.0 mg, 86 %).

^{1}H NMR (500 MHz, $CDCl_3$): δ 9.49 – 9.34 (m, 3H), 7.65 – 7.40 (m, 12H), 7.26 – 7.21 (m, 5H), 7.20 – 7.12 (m, 6H), 7.04 (dd, *J* = 8.5, 5.2 Hz, 2H), 6.96 (dd, *J* = 8.5, 4.1 Hz, 2H), 6.88 – 6.75 (m, 6H), 6.43 – 6.27 (m, 3H), 2.11 (d, *J* = 18.6 Hz, 9H), 0.89 – 0.65 (m, 9H), -0.15 – -0.37 (m, 6H).

^{13}C NMR (126 MHz, $CDCl_3$): δ 177.50, 177.27, 172.42, 172.00, 163.42, 163.19, 157.34, 156.86, 141.77, 136.72, 136.49, 136.27, 136.07, 133.13, 132.99, 129.46, 128.19, 125.24, 123.54, 123.05, 122.87, 120.77, 120.64, 117.00, 106.06, 77.21, 20.56, 10.23, 10.12.

(APPI-MS): *m/z* $[M+H]^+$: calculated 1225.43; **found 1225.44**

Synthesis of Mono-Al-Salophen Complex **L2(AlEt)**
To a suspension of **L2** (150 mg, 0.37 mmol) in toluene (12 ml), a solution of $AlEt_3$ (42.2 mg, 0.37 mmol) in toluene (4 ml) was added dropwise. The solution was stirred at room temperature overnight before being concentrated *in vacuo* to yield a yellow solid (158.0 mg, 92%).

^{1}H NMR (500 MHz, $CDCl_3$): δ 8.67 (s, 1H), 7.55 – 7.41 (m, 5H), 7.36 (dd, *J* = 7.8, 1.9 Hz, 1H), 7.27 – 7.16 (m, 4H), 7.14 – 7.07 (m, 2H), 6.88 (ddd, *J* = 8.6, 7.4, 1.3 Hz, 1H), 6.82 – 6.75 (m, 2H), 6.43 (dd, *J* = 8.4, 1.2 Hz, 1H), 2.11 (s, 3H), 0.68 (t, *J* = 8.1 Hz, 3H), -0.16 – -0.47 (m, 2H).

^{13}C NMR (126 MHz, $CDCl_3$): δ 174.02, 167.23, 164.80, 160.82, 139.93, 138.88, 137.52, 136.74, 135.85, 133.61, 132.93, 129.49, 129.04, 128.75, 128.23, 127.40, 127.08, 125.30, 124.89, 124.12, 123.12, 122.95, 119.73, 119.17, 116.77, 116.42, 20.51, 10.03, 1.02.

(APPI-MS): *m/z* $[M+H]^+$: calculated 461.17; **found 461.18**

Supporting Information

The authors have cited additional experimental and characterisation data within the Supporting Information.[14, 19, 45-48]

Acknowledgements

We gratefully acknowledge the EPSRC SOFI^2 Centre for Doctoral Training (P. L. EP/S023631/1), MARA Malaysia (M. A. R.), the UKRI Future Leaders Fellowship (J. A. G. MR\T042710\1), British Ramsay Memorial Trust (J. A. G.), L'Oréal-UNESCO for Women in Science UK & Ireland Fellowship (J. A. G.) and British Royal Society (J. A. G. RSG\R1\180101) for funding. We would also like to thank the Edinburgh Computing and Data Facility for access to high performance computing resources, and Professor Michael Ingleson for useful discussions.

Keywords: Multimetallic cooperativity • Aluminium • Ring-opening polymerization • Cyclic esters

[1] N. Sträter, W. N. Lipscomb, *Angew. Chem. Int.l Ed. Engl.* **1996**, *35*, 2024–2055.
[2] M. J. Stanford, A. P. Dove, *Chem. Soc. Rev.* **2010**, *39*, 486–494.
[3] W. Gruszka, J. A. Garden, *Nat. Commun.* **2021**, *12*, 1–13.
[4] R. Mehta, V. Kumar, H. Bhunia, S. N. Upadhyay, *J. Macromol. Sci. Polym. Rev.* **2005**, *45*, 325–349.
[5] C. M. Thomas, *Chem. Soc. Rev.* **2010**, *39*, 165–173.
[6] M. Okada, *Prog. Polym. Sci.* **2002**, *27*, 87–133.
[7] C. K. Williams, *Chem. Soc. Rev.* **2007**, *36*, 1573–1580.
[8] L. J. Wu, W. Lee, P. Kumar Ganta, Y. L. Chang, Y. C. Chang, H. Y. Chen, *Coord. Chem. Rev.* **2023**, *475*, 214847.
[9] N. Nomura, R. Ishii, Y. Yamamoto, T. Kondo, *Chem. A Eur. J.* **2007**, *13*, 4433–4451.
[10] P. Hormnirun, E. L. Marshall, V. C. Gibson, R. I. Pugh, A. J. P. White, *Proc. Natl. Acad. Sci. U. S. A.* **2006**, *103*, 15343–15348.
[11] A. J. Gaston, Z. Greindl, C. A. Morrison, J. A. Garden, *Inorg. Chem.* **2021**, *60*, 2294–2303.
[12] F. Isnard, M. Lamberti, L. Lettieri, I. D'Auria, K. Press, R. Troiano, M. Mazzeo, *Dalton. Trans.* **2016**, *45*, 16001–16010.
[13] T. Shi, Q. De Zheng, W. W. Zuo, S. F. Liu, Z. B. Li, *Chin. J. Polym. Sci. (Engl. Ed.)* **2018**, *36*, 149–156.
[14] X. Pang, R. Duan, X. Li, C. Hu, X. Wang, X. Chen, *Macromolecules* **2018**, *51*, 906–913.
[15] S. R. Kosuru, F. J. Lai, Y. L. Chang, C. Y. Li, Y. C. Lai, S. Ding, K. H. Wu, H. Y. Chen, Y. H. Lo, *Inorg. Chem.* **2021**, *60*, 10535–10549.
[16] R. Duan, C. Hu, Z. Sun, H. Zhang, X. Pang, X. Chen, *Green Chem.* **2019**, *21*, 4723–4731.
[17] R. Duan, Y. Zhou, Y. Huang, Z. Sun, H. Zhang, X. Pang, X. Chen, *Chem. Commun.* **2021**, *57*, 133–136.
[18] A. K. Asatkar, M. Tripathi, D. Asatkar, in *Stab. Appl. Coord. Compd.* (Ed.: A.N. Srivastva), IntechOpen, Rijeka, **2020**, pp. 99–104.
[19] C. G. Freiherr Von Richthofen, A. Stammler, H. Bögge, T. Glaser, *J. Org. Chem.* **2012**, *77*, 1435–1448.
[20] C. Baleizão, H. Garcia, *Chem. Rev.* **2006**, *106*, 3987–4043.
[21] S. Dayagi, Y. Degani, in *Carbon–Nitrogen Double Bond.*, John Wiley & Sons, Ltd, **1970**, pp. 61–147.
[22] A. W. Kleij, *Eur. J. Inorg. Chem.* **2009**, 193–205.
[23] T. Glaser, M. Heidemeier, R. Fröhlich, P. Hildebrandt, E. Bothe, E. Bill, *Inorg. Chem.* **2005**, *44*, 5467–5482.
[24] P. Saxena, R. Murugavel, *J. Chem. Sci.* **2017**, *129*, 1499–1512.
[25] B. Feldscher, A. Stammler, H. Bögge, T. Glaser, *Dalton. Trans.* **2010**, *39*, 11675–11685.
[26] T. Glaser, *Coord. Chem. Rev.* **2013**, *257*, 140–152.
[27] C. Mukherjee, A. Stammler, H. Bögge, T. Glaser, *Chem. A Eur. J.* **2010**, *16*, 10137–10149.
[28] A. W. Addison, T. N. Rao, J. Reedijk, J. van Rijn, G. C. Verschoor, *J. Chem. Soc., Dalton. Trans.* **1984**, 1349–1356.
[29] A. Rae, A. J. Gaston, Z. Greindl, J. A. Garden, *Eur. Polym. J.* **2020**, *138*, 109917.
[30] A. Kowalski, A. Duda, S. Penczek, *Macromolecules* **1998**, *31*, 2114–2122.
[31] E. Fazekas, P. A. Lowy, M. Abdul Rahman, A. Lykkeberg, Y. Zhou, R. Chambenahalli, J. A. Garden, *Chem. Soc. Rev.* **2022**, *51*, 8793–8814.
[32] Y. Wei, S. Wang, S. Zhou, *Dalton. Trans.* **2016**, *45*, 4471–4485.

[33] W. Gruszka, L. C. Walker, M. P. Shaver, J. A. Garden, *Macromolecules* **2020**, *53*, 4294–4302.
[34] D. Jędrzkiewicz, G. Adamus, M. Kwiecień, Ł. John, J. Ejfler, *Inorg. Chem.* **2017**, *56*, 1349–1365.
[35] H. C. Tseng, M. Y. Chiang, W. Y. Lu, Y. J. Chen, C. J. Lian, Y. H. Chen, H. Y. Tsai, Y. C. Lai, H. Y. Chen, *Dalton. Trans.* **2015**, *44*, 11763–11773.
[36] S. Ghosh, Y. Schulte, C. Wölper, A. Tjaberings, A. H. Gröschel, G. Haberhauer, S. Schulz, *Organometallics* **2022**, *41*, 2698–2708.
[37] L. Chen, W. Li, D. Yuan, Y. Zhang, Q. Shen, Y. Yao, *Inorg. Chem.* **2015**, *54*, 4699–4708.
[38] X. Ma, M. Yao, M. Zhong, Z. Deng, W. Li, Z. Yang, H. W. Roesky, *Z. Anorg. Allg. Chem.* **2017**, *643*, 198–202.
[39] Y. Zhou, G. S. Nichol, J. A. Garden, *Eur. J. Inorg. Chem.* **2022**, *16*, 1–8.
[40] H. C. Huang, B. Wang, Y. P. Zhang, Y. S. Li, *Polym. Chem.* **2016**, *7*, 5819–5827.
[41] C. Jacobs, *Macromolecules* **1993**, *26*, 6378–6385.
[42] F. M. García-Valle, R. Estivill, C. Gallegos, T. Cuenca, M. E. G. Mosquera, V. Tabernero, J. Cano, *Organometallics* **2015**, *34*, 477–487.
[43] M. Save, A. Soum, *Macromol. Chem. Phys.* **2002**, *203*, 2591–2603.
[44] J. H. Chong, M. Sauer, B. O. Patrick, M. J. MacLachlan, *Org. Lett.* **2003**, *21*, 3823–3826.
[45] G. M. Sheldrick, *Acta Crystallogr. Sect. C* **2015**, *71*, 3–8.
[46] O. V. Dolomanov, L. J. Bourhis, R. J. Gildea, J. A. K. Howard, H. Puschmann, *J. Appl. Crystallogr.* **2009**, *42*, 339–341.
[47] T. M. Ovitt, G. W. Coates, *J. Am. Chem. Soc.* **2002**, *124*, 1316–1326.
[48] D. H. Wu, A. Chen, C. S. Johnson, *J. Magn. Reson. Ser. A* **1995**, *115*, 260–264.

Entry for the Table of Contents

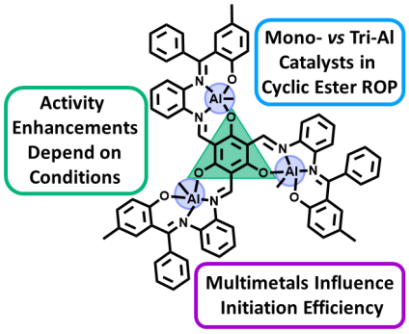

Multimetallic catalysts are gaining traction as they can deliver activity enhancements due to “cooperative” effects, yet the origins of cooperativity are not always well understood. Here, two trimetallic Al complexes and their monometallic analogues are synthesised, characterised and employed as catalysts in cyclic ester ring-opening polymerisation, providing spectroscopic and kinetic insights into the reasons behind the performance enhancements observed.

Institute and/or researcher Twitter usernames: @garden_jenni, @PhoebeLowy, @gardengroupchem and @EdinburghChem

Jenni Garden received her MSci (1st Class Hons, 2010) and PhD (2014) from the University of Strathclyde, the latter under the direction of Prof. Robert Mulvey. This was followed by two years as a postdoctoral researcher in the group of Prof. Charlotte Williams at Imperial College London. In 2016, Jenni moved to the University of Edinburgh as the first recipient of the Christina Miller Research Fellowship, which was followed by a Ramsay Memorial Trust Fellowship (2018-2020), L'Oréal-UNESCO for Women in Science UK & Ireland Fellowship (2019) and UKRI Future Leaders Fellowship (2020-present).